

1 **CD14 MODULATES PI3K/AKT/p38-MAPK “LICENSING” OF NEGATIVE REGULATORS OF TLR**
2 **SIGNALING TO RESTRAIN CHRONIC INFLAMMATION**

3
4 Bikash Sahay¹, Rebeca L. Patsey¹, Nicole Whatley¹, Sasmita Nayak^{1,2}, Christian H. Eggers^{3,4},
5 Justin D. Radolf^{5,6}, and Timothy J. Sellati^{1*}

6
7 ¹Center for Immunology and Microbial Disease, Albany Medical College, Albany, NY 12208

8 ²Present address: Department of Biology, Rensselaer Polytechnic Institute, Troy, NY 12180

9 ³Department of Medicine, University of Connecticut Health Center, Farmington, CT 06030

10 ⁴Present address: Department of Biomedical Sciences, Quinnipiac University, Hamden, CT 06518

11 ⁵Departments of Medicine and ⁶Genetics and Developmental Biology, University of Connecticut Health Center,
12 Farmington, CT 06030

13
14 Correspondence should be addressed to Dr. Timothy J. Sellati, Center for Immunology and Microbial Disease,
15 Albany Medical College, 47 New Scotland Avenue, MC151, ME205B, Albany, NY 12208-3479. Telephone:
16 (518) 262-8140, Fax: (518) 262-2885, E-mail address: sellatt@mail.amc.edu

17
18 **Nonstandard abbreviations used:** MEMs, microbe expressed structural molecules; MOI, multiplicity of
19 infection; p.i., post-infection; qRT-PCR, quantitative real-time PCR.

20
21 **Key words:** Bacterial, Monocytes/macrophages, Cell Surface Molecules, Signal Transduction

1 **ABSTRACT**

2 Current thinking emphasizes the primacy of CD14 in facilitating TLR recognition of microbes to initiate
3 proinflammatory signaling events and the importance of p38-MAPK in augmenting such responses. Herein,
4 this paradigm is challenged by demonstrating that recognition of *Borrelia burgdorferi* not only triggers an
5 inflammatory response in the absence of CD14, but one that is uncontrolled as a consequence of impaired
6 PI3K/AKT/p38-MAPK signaling and negative regulation of TLR2. CD14 deficiency results in
7 hyperphosphorylation of AKT and reduced activation of p38. Such aberrant signaling leads to decreased
8 negative regulation by SOCS1, SOCS3, and CIS thereby engendering a more severe and persistent
9 inflammatory response to *B. burgdorferi*. Perturbation of this CD14/p38-MAPK-dependent mechanism of
10 immune regulation may underlie development of infectious chronic inflammatory syndromes.

1 Toll-like receptor (TLR) signaling orchestrates innate response to the microbe-expressed molecular
2 structures (MEMS) associated with pathogens. The principal proinflammatory MEMS of the human spirochetal
3 pathogen *Borrelia burgdorferi*, the causative agent of Lyme disease, are triacylated lipoproteins recognized by
4 heterodimers of TLR2 and TLR1¹. Such recognition by TLR2 activates the NF- κ B, MAPK, and PI3K/AKT
5 pathways which coordinately regulate inflammation-associated gene activities responsible for host defense².
6 Although many aspects of Lyme disease pathogenesis remain ill-defined, it generally is accepted that clinical
7 manifestations result primarily, perhaps entirely, from the host's local immune response to spirochetes³.

8 CD14, a GPI-anchored protein expressed by macrophages (M Φ) and neutrophils, facilitates TLR-
9 dependent proinflammatory cytokine production. Mice deficient for CD14 and their M Φ exhibit
10 hyporesponsiveness when exposed to MEMS in the form of a bacterial lysate or purified agonists such as LPS,
11 lipoproteins, and their synthetic analogs⁴⁻⁶. This hyporesponsiveness has been attributed to (i) the lower affinity
12 of non-CD14-complexed LPS for TLR4⁷, (ii) the requirement for CD14 in MyD88-independent signaling⁸,
13 and/or (iii) the inability of p38, a member of the serine/threonine MAPK family, to be induced in the absence of
14 CD14⁹. Reviewing the literature one might conclude that CD14 is indispensable for elaboration of an
15 inflammatory response to its cognate MEMS⁴⁻⁶. Surprisingly, however, both *in vitro* and *in vivo* recognition of
16 several pathogens (e.g., *Borrelia burgdorferi*, *Staphylococcus aureus*, *Salmonella typhimurium*, and
17 *Streptococcus* or *Klebsiella pneumoniae*) in the absence of CD14 leads to exaggerated proinflammatory
18 cytokine production and worsening disease¹⁰⁻¹³.

19 Following exposure of host cells to pathogens or their isolated constituents, p38 is activated through
20 phosphorylation¹⁴. The action of p38 drives maturation of the phagosome following microbial uptake¹⁵,
21 activates downstream kinases that result in the translocation of NF- κ B¹⁶, stabilizes mRNA encoding
22 cytokines¹⁷, and activates genes encoding suppressors of cytokine signaling 3 (SOCS3) which negatively
23 regulates pathogen-induced inflammation¹⁸. Because the pleiotropic action of p38 is thought to augment
24 inflammation, the pharmaceutical industry has actively pursued development of potent and specific p38
25 inhibitors for the treatment of various inflammatory disorders¹⁴. However, it has been reported that inhibition
26 of p38 both *in vitro* and *in vivo* results in higher cytokine production and more severe disease in a mouse model

1 of pneumococcal pneumonia and tuberculosis¹⁹. More recently, inhibition of p38 has been linked with
2 sustained expression of TNF receptor-1, which perpetuates TNF- α induced NF- κ B signaling²⁰.

3 Herein we advance a mechanistic explanation for these dichotomous findings which distinguishes
4 CD14-dependent from -independent signaling and recognition of live *B. burgdorferi* versus lysed spirochetes.
5 Using a murine model of Lyme borreliosis we show that CD14 deficiency results in (i) dysregulation of the
6 PI3K/AKT/p38-MAPK pathway, (ii) loss of negative regulation of TLR2 signaling, (iii) increased cytokine
7 production, and (iv) inefficient clearance of bacteria by M Φ . *In vitro* studies of cytokine response of CD14^{+/+}
8 and CD14^{-/-} cells to live spirochetes reveal that inhibition of p38 augments the TNF- α response, and ablates the
9 response to lysed organisms. Collectively, our results support the rather provocative notion that CD14 signaling
10 is essential for prolonged p38 activation and thus clearance of bacteria as well as resolution of inflammation.
11 Importantly therapeutic benefit derived from p38 inhibition in certain models of inflammation (e.g., rheumatoid
12 arthritis)¹⁴ may potentiate inflammatory processes under other circumstances (e.g. Lyme arthritis).

1 RESULTS

2 **CD14 deficiency augments TLR-dependent gene activity.** *B. burgdorferi*-induced activation of CD14^{-/-} MΦ
3 results in greater transcription, persistent surface expression of TLR2, and a concomitant increase in
4 proinflammatory cytokine production, particularly TNF-α, compared to CD14^{+/+} cells¹². To more broadly
5 evaluate the impact of CD14 deficiency on the inflammatory transcriptome of MΦ, we measured transcription
6 of 84 genes associated with TLR signaling. Compared to cells expressing CD14, greater transcription of
7 interleukins (i.e., IL-1α, IL-1β, IL-2, IL-6, IL-12, IFN-γ), chemokines (i.e., CCL-2), growth factors (i.e., G-
8 CSF), and proinflammatory lipid mediators (i.e., COX2) was observed in CD14^{-/-} MΦ at 24 h p.i. (**Fig 1a**).
9 TLR2 transcript levels, but not those of other TLRs, were elevated 50-fold in CD14^{-/-} MΦ compared to wild-
10 type cells. Also, much of the dysregulated gene activity in the former cells was associated with the NF-κB
11 signaling pathway. In CD14^{+/+} MΦ gene induction peaked at 3 h and returned to baseline by 24 h p.i.; in
12 contrast, general gene activity was greater in CD14^{-/-} cells at 3 h and remained elevated throughout the course of
13 the experiment (data not shown) suggesting a critical role for CD14 in downmodulation of inflammatory
14 signaling.

15
16 ***B. burgdorferi* fails to trigger the expression of negative regulators of TLR signaling in the absence of**
17 **CD14.** Negative regulators of TLR signaling include soluble (s) molecules (e.g., sMyD88 and sTLRs),
18 competitive inhibitors (e.g., IRAKM), protein phosphatases [e.g., MAPK phosphatase 1, (MKP1)], E3 ligases
19 (e.g., SOCSs), etc.²¹. The above findings prompted an evaluation of the impact of CD14 deficiency on several
20 of these negative regulators. *B. burgdorferi* induced significantly higher transcription of *socs1* (~3.5-fold) in
21 CD14^{+/+} MΦ than in their CD14^{-/-} counterparts by 6 h p.i. ($P < 0.05$) (**Fig. 1b**). Similarly, increased expression
22 of SOCS-1 protein was observed in CD14^{+/+} MΦ, whereas no expression was detected in their CD14-deficient
23 counterparts (**Fig. 1c**). *Socs3* transcription also was greater in CD14^{+/+} MΦ compared to CD14^{-/-} cells (~3.5-
24 fold at three h and ~2.5-fold at six h) ($P < 0.01$) (**Fig. 1b**). Owing to rapid proteasome-mediated degradation of
25 SOCS3, this molecule only can be detected by Western blot analysis with addition of the proteasome inhibitor,

1 MG132 (10 μ M), for one h prior to collection of M Φ co-incubated with *B. burgdorferi* for the specified time
2 periods. Under these conditions, SOCS3 expression peaked in CD14^{+/+} cells at six h whereas no expression was
3 detected in M Φ lacking CD14 (**Fig. 1c**). CD14^{+/+} cells also exhibited *cis* gene activity ~5.6-fold above that seen
4 in CD14^{-/-} M Φ ($P > 0.01$) (**Fig. 1b**). At its peak, *cis* transcript levels in wild-type cells were ~400-fold over
5 mock controls. By 24 h p.i. transcription of these negative regulators in CD14^{+/+} and CD14^{-/-} M Φ was
6 indistinguishable and transcription of *mkp1* and *irakm* was not significantly different in these cells at any time
7 point studied (**Supplementary Fig 1**, online). Thus negative regulation of TLR signaling depends, at least in
8 part, on CD14.

9
10 **CD14 signaling regulates the activation state of IRF and STAT molecules.** To elucidate why transcription
11 of *socs1* and *socs3* is diminished in CD14^{-/-} cells, we examined the expression of three transcription factors
12 known to either directly or indirectly regulate their transcription^{22, 23}. *B. burgdorferi* induced ~13-fold higher
13 transcription of *irf1* in CD14^{+/+} M Φ than in unstimulated controls ($P < 0.05$) (**Fig. 2a**). Transcription of both
14 *irf7* and *stat1* was significantly higher in CD14^{-/-} M Φ than in wild-type cells at 24 h (**Fig 2a**), whereas no
15 differences were seen for *irf3*, *stat3*, or *stat4* (**Supplementary Fig 1**, online). Additionally, Western blot
16 analysis revealed that phospho-STAT1, but not phospho-STAT3, levels were higher in CD14^{+/+} than in CD14^{-/-}
17 M Φ (**Fig. 2b**). Diminished SOCS expression in CD14^{-/-} M Φ is consistent with the observed reduction in
18 transcriptional activation of *irf1* and STAT1 phosphorylation.

19
20 **The inflammatory response to *B. burgdorferi* is perpetuated in the absence of CD14.** The mouse model of
21 Lyme borreliosis was used to elucidate the relationship between CD14 signaling, SOCS activity, and disease
22 progression. Arthritis, an inflammatory hallmark of Lyme disease, is a self-limiting process in mice that peaks
23 between 2 and 3 weeks p.i. and typically resolves by 6 weeks²⁴. As previously reported for tick-mediated
24 infection¹², syringe inoculation of mice with *B. burgdorferi* resulted in tibiotarsal joint swelling (reflective of
25 synovitis/arthritis with periarticular edema) in CD14^{+/+} and CD14^{-/-} mice which peaked at 2 weeks p.i..
26 Contrary to CD14^{-/-} joints, joint inflammation in the wild-type mice resolved by 3 weeks p.i. (**Fig. 3a**).

1 Beginning at 2 weeks p.i. and continuing for the duration of the experiment, the joints of CD14^{-/-} mice were
2 significantly more inflamed ($P > 0.001$). Consistent with more severe and prolonged joint inflammation in
3 CD14^{-/-} mice (**Fig. 3a**), transcription of *socs1* and *socs3* in joint tissue was greatly reduced compared to wild-
4 type mice (**Fig. 3b**), as was the transcription of *cis* and *irakM* (data not shown).

5 One might predict a superior capacity to clear spirochetes in *B. burgdorferi*-infected CD14^{-/-} mice by
6 virtue of greater cytokine production (e.g., TNF- α and IFN- γ) (**Fig 7 and ref 12**). Surprisingly, all organs
7 recovered from CD14^{-/-} mice, with the exception of the heart, had heavier bacterial burdens than those of wild-
8 type animals (**Fig. 3c**). Taken together, these data suggest an indispensable role for CD14-dependent signaling
9 in negative regulation of inflammation, clearance of bacteria, and disease resolution.

11 **Killing, but not internalization, of *B. burgdorferi* by M Φ is significantly impaired in the absence of CD14.**

12 A report that CD14 acts as a unique phagocytic receptor for Gram-negative bacteria²⁵ suggests this molecule
13 may serve a similar function in spirochetal uptake. In light of the inverse relationship between expression of
14 CD14 and spirochetal burden in infected tissues, we examined the impact of CD14 deficiency on phagocytosis
15 *B. burgdorferi*. GFP-expressing spirochetes were internalized as readily by CD14^{-/-} M Φ as by those expressing
16 CD14 (**Fig. 4a**). Furthermore, neither the kinetics of internalization (**Fig. 4b**), nor the number of bacteria
17 associated per cell, as measured by changes in mean fluorescence intensity, was influenced by CD14 deficiency
18 (data not shown).

19 Killing of bacteria within the phagolysosomal compartment depends, at least in part, on the production
20 of RNS/ROS²⁶. Although differences in uptake were not observed, the ultimate fate of *B. burgdorferi*
21 internalized by CD14^{+/+} and CD14^{-/-} M Φ might differ. Indeed, assessing gene activity both *in vitro* and *in vivo*
22 it was observed that *inos* transcript levels were significantly higher in the cells from and the joints of CD14^{+/+}
23 mice (**Fig. 4c**). These differences were reflected in two-fold more cultivable spirochetes being recovered from
24 6 h-infected CD14^{-/-} (7,252 bacteria/ml) versus CD14^{+/+} (3,567 bacteria/ml) M Φ as measured using a modified
25 tissue culture infective dose method.

1 **CD14 signaling regulates activation of the p38-MAPK pathway, inhibition of which leads to lower SOCS3**
2 **and higher cytokine production by MΦ.** A p38-STAT1-IRF1 signaling axis negatively regulates TLR2
3 activity while positively regulating iNOS, SOCS1, and SOCS3 activity²⁷. To determine whether CD14
4 signaling modulates this axis, the phosphorylation state of p38 was evaluated in CD14^{-/-} MΦ. In contrast to
5 cells expressing CD14, detectable levels of phospho-p38 were only observed transiently in *B. burgdorferi*-
6 stimulated CD14^{-/-} MΦ (**Fig. 5a**). This result was confirmed and extended through use of a phospho-CBA kit;
7 as seen in **Fig. 5b**, spirochetes stimulated CD14-dependent increases in the level of phospho-p38 in both a time-
8 and dose-dependent manner. In contrast, no such changes were observed in the phosphorylation state of two
9 other members of the MAPK family, ERK and JNK. Finally, it should be appreciated that given the known
10 transcriptional inhibition of *tlr2* by p38²⁷, the higher transcription of this gene seen in **Fig. 1a** and expression of
11 TLR2 on CD14^{-/-} peritoneal MΦ is entirely consistent with the decreased phospho-p38 levels observed in CD14^{-/-}
12 MΦ (**Fig. 5a, 5b**).

13 Pharmacological inhibition of p38 has implicated this molecule in proinflammatory responses to a
14 variety of stimuli of microbial, host, and environmental origin¹⁴. Thus, the coexistence of higher phospho-p38
15 and lower cytokine production by *B. burgdorferi*-stimulated CD14^{+/+} MΦ was counterintuitive. To clarify the
16 role of p38 in our model arctigenin, a general MAPK inhibitor, and SB202190, a p38-specific inhibitor, were
17 used. These inhibitors significantly lowered the transcription of *socs3* and *inos* by CD14^{+/+} MΦ in response to *B.*
18 *burgdorferi* (**Fig. 5c**). As predicted based upon lower *socs3* transcript levels, arctigenin and SB202190 relieved
19 the inhibition of TNF- α release by wild-type cells (**Fig. 5d**) and did so in a dose-dependent fashion
20 (**Supplementary Fig 2**, online). In stark contrast, SB203580 decreased TNF- α production by cells co-
21 incubated with borrelial lysate (10 μ g/ml), (**Fig. 5e**). This latter finding is entirely consistent with the widely-
22 reported observation that p38 enhances cellular inflammatory responses to isolated bacterial MEMS^{16, 28} and
23 underscores the difference between stimulation of cells with live spirochetes as opposed to spirochetel lysates or
24 lipoproteins^{12, 16, 29, 30}.

1 **Suppression of the PI3K/AKT axis reimposes regulation of proinflammatory cytokine production by**
2 **CD14^{-/-} MΦ.** Detection of phospho-p38 for only a brief period implied strict CD14-dependent modulation of
3 this signaling cascade (**Fig. 5a**). p38-MAPK is negatively regulated through activation of AKT, a serine-
4 threonine kinase activated via PI3K³¹. The levels of phospho-AKT in CD14^{-/-} MΦ were significantly increased
5 above baseline and above that seen in cells expressing CD14 (**Fig. 6a**). Of note, peak phosphorylation of AKT
6 in CD14^{-/-} cells appeared to immediately precede disappearance of phospho-p38 (**Fig. 5a**, 10 min). The PI3K
7 inhibitors wortmannin and Ly294002 were used, to determine whether AKT activity contributing to decreased
8 phospho-p38 levels. As shown in Fig. 6B, exposure of cells to either inhibitor for 30 min prior to incubation
9 with *B. burgdorferi* eliminated the phospho-AKT pool (**Fig. 6b**). Blocking PI3K-dependent AKT function
10 should result in de-repression of p38 phosphorylation³¹. Ly294002, but not wortmannin, treatment of CD14^{-/-}
11 MΦ resulted in a further ~2-fold enhancement of p38 phosphorylation (**Fig. 6b**) following co-incubation with
12 *B. burgdorferi*. The inability of wortmannin to have the same effect as Ly294002 may be attributable to its
13 known “off target” inhibition of the p38-MAPK pathway³². To explore further how signaling through the
14 PI3K/AKT axis influences *B. burgdorferi*-induced MΦ activation, spirochetes were incubated with CD14^{-/-} cells
15 that were untreated or treated with Ly294002. Enhanced phosphorylation of p38 correlates with a profound
16 reduction in *B. burgdorferi*-induced TNF-α secretion by CD14^{-/-} MΦ whereas nearly 10-fold more TNF-α is
17 secreted in the absence of the inhibitor (**Fig. 6c**), an effect that is dose-dependent (**Supplementary Fig. 3**,
18 online).

19
20 **In the absence of CD14, *B. burgdorferi* triggers TNF-α production in both a TLR2-dependent and -**
21 **independent fashion.** Recognition that *B. burgdorferi* stimulates innate host responses primarily through
22 engagement of TLR2^{33, 34} led us to consider whether the uncontrolled release of TNF-α by CD14^{-/-} MΦ
23 correlates with their dramatically increased expression of TLR2 (**Fig. 1a** and **Ref. 12**). To answer this question,
24 mice deficient for CD14 or TLR2 (each backcrossed 10 generations onto a C3H/HeN background) were crossed
25 to establish animals homozygous recessive for both loci. MΦ expressing CD14 and TLR2 and those deficient
26 for individual or both loci were co-incubated with *B. burgdorferi* and TNF-α levels were measured (**Fig 7**). In

1 the absence of CD14, TNF- α production was significantly higher compared to their wild-type counterparts at 24
2 hp.i.. TLR2 deficiency had the opposite effect insofar as TNF- α release was significantly reduced compared to
3 wild-type M Φ at 6 h and 24 h p.i.. Remarkably, the cell's capacity to secrete TNF- α in the absence of both
4 CD14 and TLR2 was partially or fully restored to the levels released by CD14^{-/-} and wild-type M Φ ,
5 respectively. This finding is very significant as it demonstrates that, despite similarities in the exaggerated
6 Lyme disease phenotype observed in CD14^{-/-} and TLR2^{-/-} mice, these two signaling pathways are not entirely
7 synonymous.

1 DISCUSSION

2 Regulation of the host response to *B. burgdorferi* begins with CD14 recognition of lipoproteins^{12, 35}. In
3 the absence of such receptor engagement, Lyme borreliosis is typified by greater bacterial burden, more severe
4 histopathology, and dysregulated production of proinflammatory immunomodulators¹². Given that binding of
5 borrelial lipoproteins to CD14 facilitates downstream signaling through TLR2 and the cytosolic adaptor protein
6 MyD88 it is perhaps not surprising that mice deficient for these molecules also harbor more bacteria in their
7 tissues and present with more severe arthritis³⁶⁻³⁸. Despite similar pathophysiological features in *B.*
8 *burgdorferi*-infected mice lacking CD14, TLR2, or MyD88, CD14 is distinct in its ability to tightly regulate
9 cytokine production both *in vitro* and *in vivo*¹². CD14's unique role as an anti-inflammatory receptor is
10 supported further by the observation that signaling in its absence increases production of proinflammatory
11 cytokines in response to infection with *Staphylococcus aureus*¹⁰. A similar trend towards greater cytokine
12 production in response to *E. coli* bioparticles was seen with CD14^{-/-} versus CD14^{+/+} peritoneal MΦ³⁹. Finally,
13 blockade of CD14 by monoclonal antibody treatment increased tissue invasion and resulted in higher TNF-α
14 production in rabbits infected with *Shigella flexneri*⁴⁰.

15 Coordinate signaling through CD14 and TLR2 simultaneously activates NF-κB, p38-MAPK, and PI3K
16 pathways^{2, 41} to orchestrate both the initiation and resolution of inflammatory responses to *B. burgdorferi*.
17 CD14 deficiency, however, leads to excessive phosphorylation of AKT along with higher transcription and
18 surface expression of TLR2¹². Given that TLR2 signaling regulates PI3K activity and leads to AKT activation,
19 we were led to consider that either elevated TLR2 expression and/or higher phospho-AKT levels in CD14^{-/-} MΦ
20 underlie the more severe and persistent course of Lyme borreliosis in these mice. Cytokine release by *B.*
21 *burgdorferi*-activated MΦ deficient for both CD14 and TLR2 was comparable to that of wild-type cells, but was
22 significantly greater than that observed with TLR2^{-/-} cells and less than that of CD14^{-/-} cells. This finding
23 suggests only a partial role for TLR2 in recognition of *B. burgdorferi*, one that is strictly proinflammatory, and
24 implies the existence of another receptor(s) for bacterial recognition in the absence of CD14.

25 One candidate non-TLR receptor is complement receptor 3 (CR3), a member of the β2-integrin family
26 of adhesion molecules⁴². Using CHO cells transfected with CD14, TLR2, and CR3 in various combinations it

1 was revealed that the “inside-out” signaling responsible for increasing the avidity of CR3 for its ligand requires
2 both CD14 and TLR2⁴³. Similarly, antibodies directed against CD14 and/or TLR2 were shown to block
3 “inside-out” signaling required for CR3-mediated recognition of *Porphyromonas gingivalis* fimbriae⁴⁴. Moore
4 and coworkers reported that inhibition of CR3 signaling reduced by 50% the *E. coli*-stimulated secretion of
5 TNF- α by CD14^{-/-} peritoneal M Φ ³⁹. These various studies also implicate CR3 in uptake of bacteria^{39, 43, 44}.
6 Like CD14, this phagocytic receptor resides within the lipid raft and clustering of CR3 precedes PI3K-mediated
7 phosphorylation and activation of AKT⁴². In light of the ability of CR3 to mediate internalization of *B*
8 *burgdorferi* (personal communication, Juan Anguita, Veterinary & Animal Sciences, University of
9 Massachusetts, Amherst) and its capacity to activate PI3K, it is intriguing to speculate on whether CR3 is a
10 phagocytic receptor in the absence of CD14 whose action may account for higher cytokine production during
11 infection. Such a role is supported by the fact that spirochetal uptake was not diminished in the absence of
12 CD14.

13 AKT has pleiotropic effects that include promotion of cell survival, NF- κ B activation, and inhibition of
14 ASK1, a MAPKKK responsible for p38 activity^{31, 45}. p38 activity is associated with NF- κ B activation and
15 stabilization of mRNA encoding proinflammatory cytokines such as TNF- α ¹⁷. That inhibition of PI3K
16 prevented phosphorylation of AKT and thus increased p38 activity in *B. burgdorferi*-activated CD14^{-/-} M Φ is
17 consistent with the inverse relationship between AKT and p38 activity. Unexpectedly, however, PI3K
18 inhibition also resulted in decreased TNF- α production, a finding inconsistent with higher p38 activity and its
19 accepted role as a proinflammatory mediator¹⁴. Nevertheless, inhibition of p38 in CD14^{+/+} cells with either
20 general or specific antagonists resulted in lower *inos* and *socs3* transcription and a dose-dependent increase in
21 TNF- α production in response to *B. burgdorferi*. Contrarily, it has been reported that SB203580 inhibits TNF- α
22 release by the mouse macrophage RAW264.7 cell line in response to borrelial lysates¹⁶. One potential
23 explanation for these divergent findings is that the “context” in which bacterial MEMS are recognized (i.e., live
24 spirochetes versus lysed organisms) influences the downstream signaling cascades initiated within the host cell.
25 Consistent with this idea, treatment of CD14^{+/+} M Φ with SB203580 inhibited TNF- α production in response to
26 borrelial lysates as previously reported¹⁶. This suggests that, in conjunction with CD14 and TLR2 engagement,

1 phagocytic receptors with a differential capacity to internalize live spirochetes versus a lysate may orchestrate
2 intracellular signaling events, a notion supported by earlier studies^{12, 29}. The anti-inflammatory capacity of p38
3 is further demonstrated in mouse models of pneumococcal pneumonia and tuberculosis where its inhibition
4 results in impaired bacterial clearance and increased TNF- α production both *in vitro* and *in vivo*¹⁹. It also has
5 been established that p38 induces the shedding of TNF receptor-1 from activated cells thus dampening their
6 responsiveness to TNF- α ²⁰. The combination of increased TNF- α production and maintenance of its cognate
7 receptor on the cell surface likely contributes to the cytokine “surge” and exacerbates the pathology associated
8 with bacterial infection. Taken together, these results challenge the notion that isolated MEMS (e.g., purified
9 LPS, lipoproteins, etc.) are equivalent to the whole organisms from which they are extracted^{12, 29}. They also
10 sound a cautionary note regarding application of p38 inhibitors to treat inflammatory disorders especially those
11 of infectious-origin. Development of immunotherapeutic strategies that enhance the action of SOCS may
12 represent a more fruitful avenue in pursuit of novel anti-inflammatory drugs⁴⁶⁻⁴⁸.

13 Finally, another set of intriguing observations was the persistent arthritis and increased spirochetal-
14 burden in the tissues of CD14^{-/-} mice. Considering the importance of bacterial clearance as an element of
15 disease resolution, we evaluated CD14 as a potential phagocytic receptor for spirochetes. Consistent with the
16 findings of Moore et al. using *E. coli* bioparticles³⁹, we report that CD14 deficiency does not impair
17 internalization of spirochetes. During the process of engulfment various receptors are engaged which initiate
18 kinase and phosphatase cascades that facilitate killing of phagocytosed bacteria. Despite the equivalent
19 capacity of CD14^{+/+} and CD14^{-/-} M Φ to engulf spirochetes, activation of p38 in the CD14^{-/-} cells was transient
20 and thus insufficient, either *in vitro* or *in vivo*, to drive the transcription of *inos* and *irf1* whose gene products
21 participate in maturation of the phagosome and bacterial killing⁴⁹. The lower transcript levels of *inos* in CD14^{-/-}
22 M Φ likely are associated with decreased RNS/ROS production⁵⁰ and may contribute, at least in part, to the
23 higher bacterial burden observed in the infected tissues of these mice. In contrast to the association of IRF1
24 with early maturation of the phagosome, IRF7 induction occurs later in this process and often is linked to
25 persistence of exogenous material within the phagosomal compartment, particularly in plasmacytoid dendritic
26 cells (pDCs)⁵¹. Higher *irf7* transcription is a hallmark of activated pDCs and is necessary for the induction of

1 Type I IFN, an important element of viral and bacterial clearance⁵². Specifically, at a point when the *ifnβ* locus
2 is transcriptionally silent in *B. burgdorferi*-activated CD14^{-/-} MΦ little IRF7 mRNA is being transcribed.
3 However, like activated pDCs, later in their activation program *irf7* transcription is significantly greater in
4 CD14^{-/-} cells than their wild-type counterparts. As in activated pDCs and RAW264.7 cells, where increased
5 IRF7 coincides with an accumulation of viral antigen or purified TLR agonist (i.e., CpG ODNs)⁵¹, we propose
6 that “frustrated” clearance of borrelial antigen from the phagosomal compartment of CD14^{-/-} MΦ may drive the
7 transcription of *irf7*. A corollary of this scenario is that persistence of borrelial TLR agonists in the phagosomal
8 compartment may perpetuate inflammatory signaling through TLR2 and other receptors of TLR or non-TLR
9 origin.

10 *In toto*, we detail a critical and unanticipated role for CD14 in downmodulating TLR2-dependent and -
11 independent pathways which regulate NF-κB signaling events. CD14 exerts its influence on the intensity and
12 duration of inflammation through the PI3K/AKT/p38-MAPK axis which we propose serves as a “rheostat” to
13 provide fine regulation of NF-κB activity, the “backbone” of the host’s inflammatory response to pathogenic
14 challenge. As depicted in our model (**Fig 8**), *B. burgdorferi*-initiated inflammatory signaling in the absence of
15 CD14 stimulates greater AKT activity which enhances NF-κB signaling while at the same time suppressing p38
16 and STAT1. p38 and STAT1 are responsible for inducing IRF1 and SOCS activity which ultimately facilitates
17 spirochete clearance and/or dampens cytokine production. Thus the more severe and persistent Lyme disease
18 phenotype observed in CD14^{-/-} mice reflects the concomitant increase in NF-κB-mediated proinflammatory
19 signaling and loss of negative regulation via diminished SOCS activity. To our knowledge this is the first
20 report implicating the CD14/p38-MAPK pathway as the driving force behind anti-inflammatory responses in a
21 mouse model of bacterial infection.

1 METHODS

2 **Reagents.** Great care was taken during the preparation of all buffers and reagents to minimize contamination
3 with environmental LPS by utilizing baked (180°C for 4 h) and autoclaved glassware, disposable plasticware,
4 and pyrogen-free H₂O that also is free of DNase and RNase activity.

5
6 **Cultivation of *B. burgdorferi*.** Low-passage *B. burgdorferi* strain 297 were maintained at 23°C in Barbour-
7 Stoenner-Kelley medium containing 6% normal rabbit serum (BSK_{complete}) from Pel-Freeze Biologicals (Rogers,
8 AR) and then temperature-shifted to 37°C. Increased expression of OspC was confirmed by silver staining of
9 whole borrelial lysates separated by SDS-PAGE. *B. burgdorferi* 297 expressing green fluorescent protein were
10 cultivated in BSK_{complete} containing 400 µg/ml kanamycin and were grown at 37°C until mid- to late-logarithmic
11 phase for subsequent use in phagocytosis experiments as previously described²⁹.

12
13 **Mice and infection protocol.** Four to eight week-old C3H/HeN (CD14^{+/+}) mice (Taconic, Germantown, NY)
14 were housed in the Animal Resources Facility at Albany Medical College. Food and water were provided *ad*
15 *libitum* and all animal procedures conformed to the Institutional Animal Care and Use Committee guidelines.
16 CD14^{-/-} mice were generated as previously described⁴ and subsequently backcrossed 10 generations onto a
17 C3H/HeN background¹². TLR2^{-/-} mice were provided by Tularik Inc. (now Amgen Inc., South San Francisco,
18 CA) and generated by Deltagen Inc. (Menlo Park, CA)⁵³ and were backcrossed 10 generations onto a C3H/HeN
19 background. C3H/HeN mice deficient for CD14 and TLR2 were crossed to establish animals homozygous
20 recessive for both alleles.

21 Mice were infected via intradermal administration of 5×10^5 spirochetes over the sternum. BSK_{complete}
22 was used as a mock-infection control. At one week intervals, tibiotarsal joint thickness was measured using
23 digital calipers and bacterial burden in infected tissues was determined using isolated genomic DNA as
24 previously described¹². Total RNA also was isolated from infected tissues for qRT-PCR as described below.

1 **Isolation and differentiation of MΦ.** MΦ were isolated from the bone marrow of six to eight week-old mice.
2 Briefly, bone marrow cells recovered by flushing femurs and tibia with DMEM were incubated in tissue
3 culture-treated 25cm²-flasks (BD Falcon, BD Biosciences, San Jose, CA) overnight at 37°C with 5% CO₂ to
4 eliminate adherent fibroblasts, granulocytes, and any contaminating MΦ⁵⁴. The following day, 1 × 10⁷
5 suspension cells were maintained in 10-cm² bacteriological Petri dishes (BD-Falcon) for three days with
6 DMEM supplemented with 10% fetal bovine serum, 20% L292-cell conditioned media, 0.01% HEPES, 0.01%
7 sodium pyruvate, and 0.01% L-glutamine. Cultures were supplemented with five ml of the above-described
8 medium and seven days after isolation cell monolayers were recovered using ice-cold PBS and scraping. Single
9 cell suspensions were used immediately or frozen in liquid nitrogen with 20% FBS and 10% DMSO for use in
10 future experiments.

11
12 ***B. burgdorferi*-MΦ co-incubation.** MΦ were seeded into 6-well tissue culture-treated plates at a concentration
13 of 1 × 10⁶ cells/2 ml/well and allowed to adhere overnight. The following day, *B. burgdorferi* were enumerated
14 and re-suspended as described above. MΦ were washed twice with serum-free DMEM to remove any traces of
15 FBS and spirochetes (resuspended in DMEM + 4% autologous serum) were added at an MOI of 10 and co-
16 incubated for different time intervals at 37°C in 5% CO₂. Cells incubated with DMEM + 4% autologous serum
17 alone served as mock-infected controls.

18
19 **Analysis of bacterial association with MΦ: Fluorescence microscopic analysis.** MΦ were seeded into 8-well
20 chamber slides (Lab-TekTM II CC2 Chamber SlideTM System) at a concentration of 1 × 10⁵ cells/200μl/well and
21 allowed to adhere overnight. The following day, GFP-expressing *B. burgdorferi* were enumerated and added to
22 cell monolayers at an MOI of 10 and co-incubated for different time intervals. After co-incubation, cells were
23 washed twice with serum-free DMEM and were fixed with 4% paraformaldehyde for 30 min. GFP-expressing
24 *B. burgdorferi* were visualized by fluorescence microscopy (Olympus UIS2Series: U-MNG2 Green excitation
25 mirror unit/NIB HIGHQ FITC). **Flow cytometric analysis.** MΦ were aliquoted into five ml polystyrene round-
26 bottom tubes (BD Biosciences, Bedford, MA) at a concentration of 5 × 10⁵ cells/600μl/tube, centrifuged at 250

1 $\times g$ for 10 min followed by incubation with GFP-expressing *B. burgdorferi* resuspended in DMEM + 4%
2 autologous serum at an MOI of 10. Cells and bacteria were coincubated for different time intervals, washed
3 twice in FA buffer (BD Microbiological Systems, Sparks, MD) and fixed in FA buffer containing 4%
4 paraformaldehyde. Sample data was acquired on a BD FACSCanto™ Flow Cytometer (BD Immunocytometry
5 Systems) and results were analyzed using FlowJo software (Ashland, OR).

6
7 **Quantitative real-time PCR.** Total RNA was isolated from MΦ using the RNeasy Mini Kit (Qiagen GmbH,
8 Hilden, Germany) as per the manufacturer. The amount and purity of RNA was quantified by Biophotometer
9 (Eppendorf AG, Hamburg, Germany) and 0.5μg were used for reverse transcription of cDNA using Superscript
10 II (Invitrogen Corporation, CA, USA). cDNA (20μl) served as the template in quantitative real-time PCR (qrt-
11 PCR) analysis using Mouse TLR Signaling Pathway RT² Profiler™ PCR Arrays (Superarray Bioscience).
12 These arrays contain primer pairs for 84 genes implicated in TLR signal transduction as well as housekeeping
13 genes and controls in a 96-well microtiter plate format. This qrt-PCR methodology directly quantifies transcript
14 levels based upon the $2^{-\Delta\Delta Ct}$ method through measurement of SYBR green fluorescence using an iQ5 real-time
15 PCR detection system (Bio-Rad Laboratories, Hercules, CA).

16 For transcriptional analysis of genes not represented on the RT² Profiler™ PCR Array, qrt-PCR was
17 performed in a final volume of 25μl containing: 12.5μl of 2X SYBR green master mix (Bio-Rad Laboratories),
18 25pMol of the specific forward and reverse primers, and 0.2μl of cDNA. Primers were designed using Beacon
19 Designer version 7.0 software (PREMIER Biosoft Intl, Palo Alto, CA) and the sequences of specific primer sets
20 are provided in **Supplemental Table 1** online. Amplification conditions were 95°C (3 min) and 40 cycles of
21 95°C (15s), 55°C (40s) and 72°C (30s). All the qrt-PCR reactions were run in triplicate with no-template
22 controls (NTC) and mean *cT* values were used for all the calculations using 18S rRNA as an internal control for
23 normalization. Effects greater than a two-fold change with respect to mock control were considered significant.

24
25 **Western blot analysis.** Antibodies directed against SOCS1, SOCS3 and CIS were obtained from Santa Cruz
26 Biotechnology, Inc. (Santa Cruz, CA), antibodies against AKT, STAT1, STAT3 and p38 were obtained from

1 Cell Signaling Technology, Inc. (Danvers, MA), and antibodies against β -actin were obtained from Bethyl
2 Laboratories, Inc. (Montgomery, TX). Protein samples (25-100 μ g, depending on the target) were resolved by
3 SDS-PAGE and transferred to nitrocellulose using semi-dry transblot (Bio-Rad Laboratories, Hercules, CA).
4 The membrane was blocked with 5% non-fat milk and then incubated overnight at 4°C with primary antibody
5 (1:1000, for AKT and STATs; 1:100 for SOCS; and 1:10,000 for β -actin). Membranes were probed with HRP-
6 conjugated anti-rabbit IgG (Cell Signaling Technology) diluted 1:2000. Specific signal was developed using
7 the SuperSignal West-Dura chemiluminescent substrate (Pierce Endogen, Rockford, IL) and recorded either on
8 photographic film or using a FluorChem 7700 Chemiluminescence Imager (Alpha Innotech, San Leandro, CA).

9
10 **Cytometric bead array (CBA) for cytokine and phospho-protein analysis.** M Φ were co-incubated with *B.*
11 *burgdorferi* at various MOI and cytokine levels were measured in the recovered culture supernatant using the
12 Mouse Inflammation CBA kit and a FACSArray flow cytometer [BD Immunocytometry Systems (BDIS), San
13 Jose, CA]. Data was acquired and analyzed using BD FACSArray software and FCAP Array software, version
14 1.0 (BDIS), respectively. For phospho-protein analysis, the protein content of the samples was normalized,
15 added to a phospho-specific CBA kit, and analyzed as described above.

16
17 **Inhibition of signaling cascades by pharmacological inhibitors.** M Φ were treated with the inhibitors
18 arctigenin (1 μ M), SB202190 (0.5 μ M), SB203580 (10 μ M), wortmannin (100nM), and Ly294002 (100 μ M) for
19 30 min prior to addition of *B. burgdorferi*. In some experiments a range of inhibitor concentrations was used.
20 DMSO alone served as a control. Culture supernatants were collected for cytokine measurement and cells were
21 lysed for RNA isolation and Western blot analysis.

22
23 **Statistical analysis.** All results were expressed as mean \pm SEM and comparisons between the groups were
24 made using one-way ANOVA followed by Bonferroni's correction. Differences between control and
25 experimental groups were considered significant using $\alpha = 0.05$.

1 **ACKNOWLEDGMENTS**

2 We thank Drs. James Drake, Jonathan Harton, Karsten Hazlett (Albany Medical College, NY), and Juan
3 Anguita (University of Massachusetts, Amherst, MA) for critical review of the manuscript. Special thanks to
4 Aaloki Shah and Sally Catlett (Albany Medical College, NY) for technical support and Daniel Desrosiers
5 (University of Connecticut Health Science Center, CT) for computer graphic design. Supported by the National
6 Institutes of Health (AI054546 to TJS; AI29735 and AI38894 to JDR) and an Arthritis Foundation Investigator
7 Award to TJS.

1 **AUTHOR CONTRIBUTIONS**

2 B.S. designed the study, did and analyzed experiments and contributed to manuscript preparation; R.L.P., N. W.
3 and S. N. did and analyzed experiments; C.H.E. generated the GFP-expressing *B. burgdorferi*; J.D.R. provided
4 GFP-expressing *B. burgdorferi* and contributed to manuscript preparation; T.J.S. designed and organized the
5 study and contributed to manuscript preparation.

1 **FIGURE LEGENDS**

2

3 **Figure 1.** Higher *B. burgdorferi*-induced inflammatory gene activity is associated with lower SOCS levels in
4 CD14^{-/-} MΦ. Total RNA from CD14^{+/+} and CD14^{-/-} MΦ co-incubated with *B. burgdorferi* was analyzed by qrt-
5 PCR **(a)** for genes involved in the TLR signaling pathway or **(b)** for *socs1*, *socs3*, and *cis*. Results presented in
6 **(a)** reflect the ratio of fold changes in HPRT-normalized gene activity in CD14^{-/-} versus CD14^{+/+} MΦ. All
7 results represent mean ± SEM. **P* < 0.05, ** *P* < 0.01. **(c)** Equivalent protein amounts of lysed MΦ were
8 separated by 12% SDS-PAGE, transferred to a PVDF membrane and probed with antibodies directed against
9 SOCS1, SOCS3, CIS, or β-actin.

10

11 **Figure 2.** IRF1, IRF7 and STAT1 are differentially activated by *B. burgdorferi* in the absence of CD14. **(a)**
12 Total RNA from CD14^{+/+} and CD14^{-/-} MΦ co-incubated with *B. burgdorferi* was analyzed by qrt-PCR for *irf1*,
13 *irf7* and *stat1*. Results represent mean ± SEM. **P* < 0.05, ** *P* < 0.01. **(b)** Equivalent protein amounts of
14 lysed MΦ were separated by 12% SDS-PAGE, transferred to a nitrocellulose membrane and probed with
15 phospho-specific STAT1 or STAT3, or β-actin antibodies.

16

17 **Figure 3.** Reduced *socs* transcription is associated with impaired bacterial clearance and more severe and
18 prolonged Lyme arthritis. **(a)** CD14^{+/+} and CD14^{-/-} mice were infected with 5×10^5 *B. burgdorferi*, and
19 tibiotarsal joint thickness was measured at 1-wk intervals. The horizontal bars indicate mean thickness for each
20 group and the data are representative of two independent experiments (n=24). **(b)** Total RNA was isolated from
21 the tibiotarsal joints of CD14^{+/+} and CD14^{-/-} mice (n=6) and an equal amount of RNA was pooled from each
22 joint and 0.5 μg was used for preparing cDNA. The cDNA was analyzed by qRT-PCR to determine the *in vivo*
23 levels of *socs1* and *socs3* transcription. Data are representative of two independent experiments. **(c)** Organs
24 were collected six weeks p.i. and DNA was isolated for quantification of bacterial burden. Results represent
25 mean ± SEM. **P* < 0.05, ** *P* < 0.01, *** *P* < 0.001.

1

2 **Figure 4.** *B. burgdorferi*-induced transcription of *inos*, but not phagocytic uptake of spirochetes, is impaired by
3 CD14 deficiency. GFP-expressing *B. burgdorferi* were co-incubated with CD14^{+/+} and CD14^{-/-} MΦ for the
4 indicated times and phagocytosis was evaluated by (a) fluorescence microscopy and (b) flow cytometry. (c)
5 *inos* transcript levels were determined by qrt-PCR using RNA isolated from MΦ co-incubated with *B.*
6 *burgdorferi* or using RNA pooled from joints isolated from infected mice as described in the legend for Fig. 3.
7 Results represent mean ± SEM. **P* < 0.05, ** *P* < 0.01, *** *P* < 0.001.

8

9 **Figure 5.** CD14 deficiency results in dysregulated p38-MAPK signaling and cytokine production in response
10 to *B. burgdorferi*. (a) Equivalent protein amounts of lysed CD14^{+/+} and CD14^{-/-} MΦ co-incubated with *B.*
11 *burgdorferi* were separated by SDS-PAGE, transferred to a nitrocellulose membrane and probed with phospho-
12 p38 and β-actin antibodies. (b) MΦ were co-incubated with *B. burgdorferi* at different MOI and equal amounts
13 of total protein were used to estimate relative phosphorylated MAPK levels by phospho-specific CBA. The
14 data shown are representative of two independent experiments. (c) CD14^{+/+} MΦ were treated with DMSO
15 alone, SB202190 (0.5 μM), or arctigenin (1 μM), for 30 min prior to co-incubation with *B. burgdorferi* at an
16 MOI of 10 and total RNA was analyzed by qrt-PCR for *inos* and *socs3*. (d) CD14^{+/+} MΦ were treated as
17 described in (c), and culture supernatants were analyzed for the presence of TNF-α by CBA. (e) CD14^{+/+} MΦ
18 were treated with DMSO alone or increasing concentrations of SB203580 for 30 min prior to co-incubation
19 with *B. burgdorferi* lysate (10μg/ml). Cell-culture supernatants were collected and TNF-α levels were
20 measured by CBA. Results in (c-e) represent mean ± SEM. **P* < 0.05, ** *P* < 0.01, *** *P* < 0.001.

21

22 **Figure 6.** Inhibition of *B. burgdorferi*-induced AKT activation in CD14^{-/-} MΦ reestablishes p38 activity and
23 restores negative regulation of cytokine production. (a) Equivalent protein amounts of lysed CD14^{+/+} and
24 CD14^{-/-} MΦ co-incubated with *B. burgdorferi* were separated by SDS-PAGE, transferred to a nitrocellulose
25 membrane and probed for phospho-AKT and β-actin. The blot shown is representative of two independent
26 experiments. (b) CD14^{-/-} MΦ were treated with DMSO alone or PI3K inhibitors [wortmannin (100nM) or

1 Ly294002 (100 μ M)] for 30 min prior to co-incubation with *B. burgdorferi*. Western blots of cellular protein
2 were probed with phospho-specific AKT and p38 antibodies and then striped and reprobed for total AKT, p38,
3 and β -actin. The data shown are representative of two independent experiments. (c) CD14^{+/+} and CD14^{-/-} M Φ
4 were treated with Ly294002 (100 μ M) for 30 min prior to co-incubated with *B. burgdorferi* for three and six h.
5 Culture supernatants were collected and TNF- α levels were measured by CBA. Results represent mean \pm SEM.
6 *** $P < 0.001$.

7
8 **Figure 7.** TLR2 plays a partial role in CD14-independent cytokine production. M Φ isolated from CD14^{+/+},
9 CD14^{-/-}, TLR2^{-/-} and CD14^{-/-}/TR2^{-/-} mice were co-incubated with *B. burgdorferi* for the indicated time points,
10 cell culture supernatants were collected and TNF- α was measured by CBA. Results represent mean \pm SEM.
11 *** $P < 0.001$.

12
13 **Figure 8.** Proposed model for CD14-dependent and -independent signaling in response to infection with *B.*
14 *burgdorferi*. In the absence of CD14, greater activation of AKT inhibits p38 activity resulting in increased
15 transcription of TLR2, reduced activation of STAT1 and IRF1, and decreased induction of SOCS necessary to
16 modulate the intensity and duration of Lyme borreliosis. The size of the red circles indicates relative
17 phosphorylation status of the indicated protein and the size of the individual protein(s) is reflective of relative
18 transcript/protein levels.

19
20 **Supplementary Figure 1.** *mkp1*, *irakm*, *irf3*, *stat3* and *stat4* transcription is CD14-independent and unaltered by
21 its absence. Total RNA from CD14^{+/+} and CD14^{-/-} M Φ co-incubated with *B. burgdorferi* was analyzed by qrt-
22 PCR for *mkp1*, *irakm*, *irf3*, *stat3*, and *stat4*. Results represent mean \pm SEM.

23
24 **Supplementary Figure 2.** Inhibition of p38 or MAPK results in a dose-dependent increase of TNF- α
25 production in CD14^{+/+} cells. CD14^{+/+} M Φ were treated with DMSO or the indicated concentrations of
26 arctigenin, SB202190 or SB203580 for 30 min prior to co-incubation with *B. burgdorferi*. Cell culture

1 supernatants were collected 24 h post incubation and TNF- α levels were measured by CBA. Results represent
2 mean \pm SEM. *** $P < 0.001$.

3

4 **Supplementary Figure 3.** Inhibition of PI3K results in a dose-dependent decrease in TNF- α production by
5 CD14^{-/-} cells. CD14^{-/-} M Φ were treated with DMSO or the indicated concentration of LY294002 for 30 min
6 prior to co-incubation with *B. burgdorferi*. Cell-culture supernatants were collected 24 h post incubation and
7 TNF- α levels were measured by CBA. Results represent mean \pm SEM. *** $P < 0.001$.

8

9 **Supplementary Table 1.** Primer sequences used in qrt-PCR

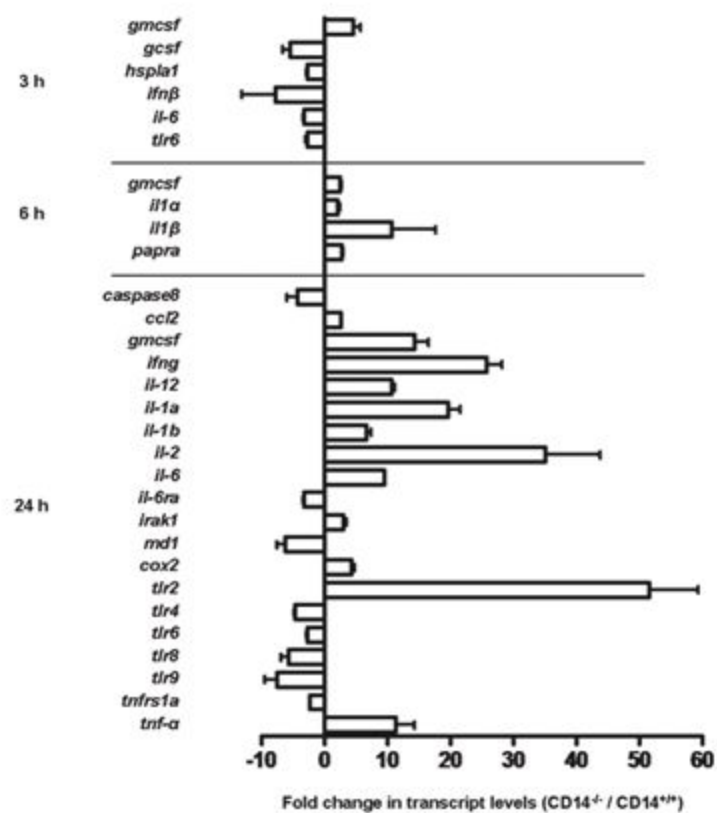
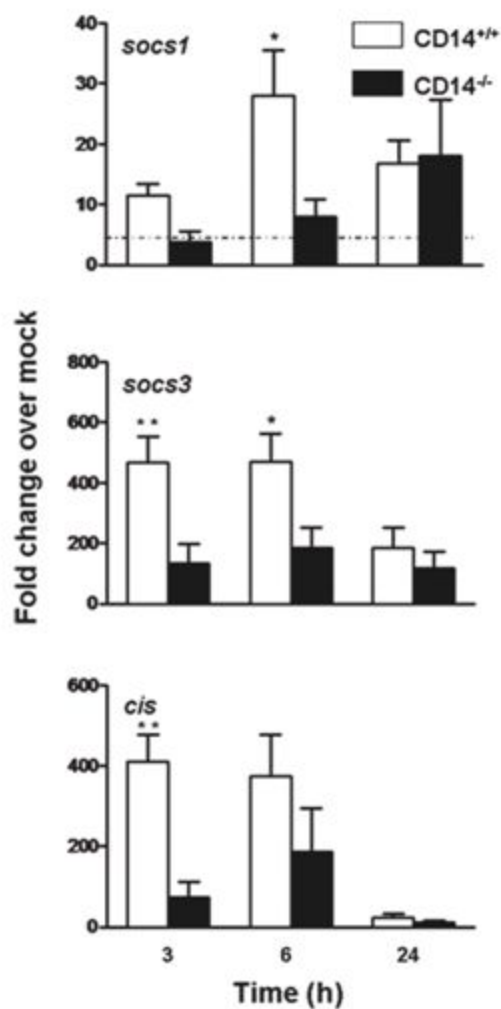
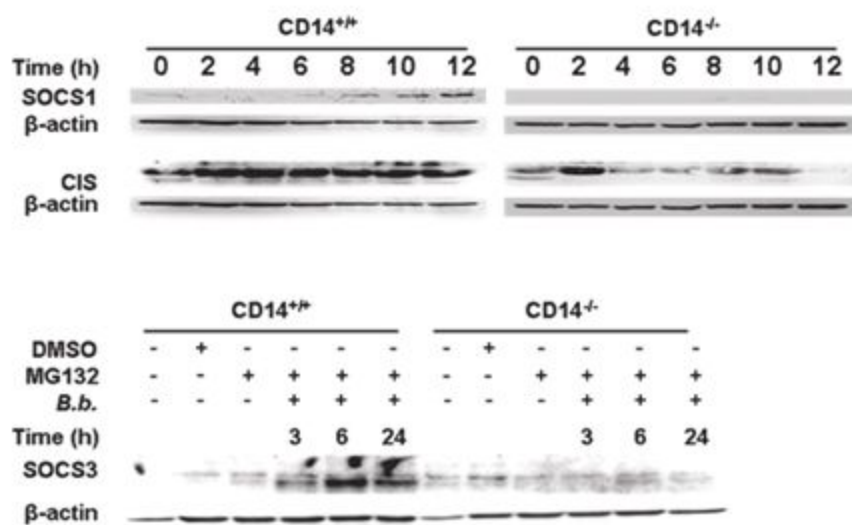
References

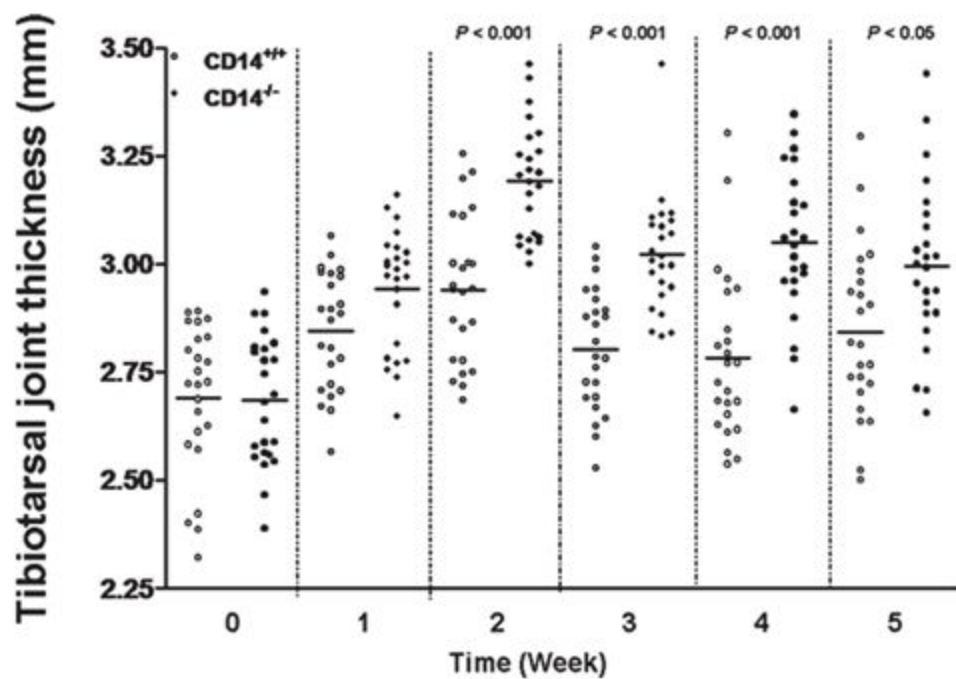
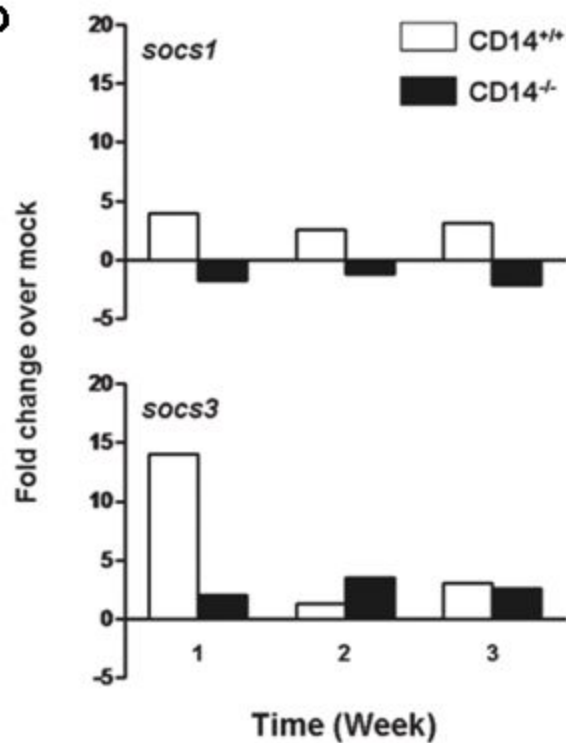
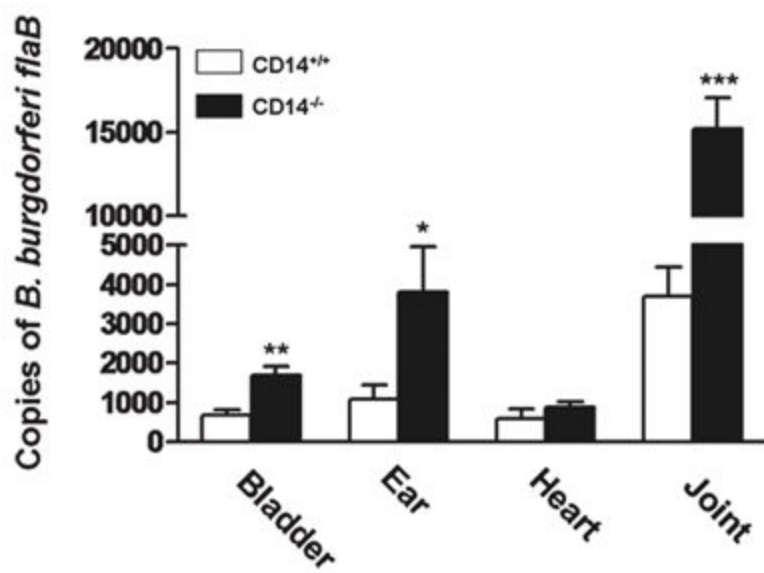
1. Wooten,R.M. & Weis,J.J. Host-pathogen interactions promoting inflammatory Lyme arthritis: use of mouse models for dissection of disease processes. *Curr. Opin. Microbiol.* **4**, 274-279 (2001).
2. Arbibe,L. *et al.* Toll-like receptor 2-mediated NF-[kappa]B activation requires a Rac1-dependent pathway. *Nat Immunol* **1**, 533-540 (2000).
3. Steere,A.C. & Glickstein,L. Elucidation of Lyme arthritis. *Nat Rev. Immunol* **4**, 143-152 (2004).
4. Haziot,A. *et al.* Resistance to endotoxin shock and reduced dissemination of gram-negative bacteria in CD14-deficient mice. *Immunity* **4**, 407-414 (1996).
5. Antal,S. Evaluation of CD14 in host defence. *European Journal of Clinical Investigation* **30**, 167-179 (2000).
6. Sellati,T.J. *et al.* Treponema pallidum and Borrelia burgdorferi lipoproteins and synthetic lipopeptides activate monocytic cells via a CD14-dependent pathway distinct from that used by lipopolysaccharide. *J Immunol* **160**, 5455-5464 (1998).
7. Landmann,R., Muller,B., & Zimmerli,W. CD14, new aspects of ligand and signal diversity. *Microbes. Infect.* **2**, 295-304 (2000).
8. Jiang,Z. *et al.* CD14 is required for MyD88-independent LPS signaling. *Nat Immunol* **6**, 565-570 (2005).
9. Han,J., Lee,J.D., Bibbs,L., & Ulevitch,R.J. A MAP kinase targeted by endotoxin and hyperosmolarity in mammalian cells. *Science* **265**, 808-811 (1994).
10. Haziot,A. *et al.* CD14 plays no major role in shock induced by Staphylococcus aureus but down-regulates TNF-alpha production. *J Immunol* **162**, 4801-4805 (1999).
11. Heumann,D., Lauener,R., & Ryffel,B. The dual role of LBP and CD14 in response to Gram-negative bacteria or Gram-negative compounds. *J Endotoxin. Res.* **9**, 381-384 (2003).
12. Benhnia,M.R. *et al.* Signaling through CD14 attenuates the inflammatory response to Borrelia burgdorferi, the agent of Lyme disease. *J Immunol* **174**, 1539-1548 (2005).
13. Echchannaoui,H. *et al.* CD14 deficiency leads to increased MIP-2 production, CXCR2 expression, neutrophil transmigration, and early death in pneumococcal infection. *J Leukoc Biol* **78**, 705-715 (2005).
14. Schieven,G.L. The biology of p38 kinase: a central role in inflammation. *Curr. Top. Med. Chem.* **5**, 921-928 (2005).
15. Blander,J.M. & Medzhitov,R. Regulation of phagosome maturation by signals from toll-like receptors. *Science* **304**, 1014-1018 (2004).
16. Olson,C.M. *et al.* p38 mitogen-activated protein kinase controls NF-kappaB transcriptional activation and tumor necrosis factor alpha production through RelA phosphorylation mediated by mitogen- and stress-activated protein kinase 1 in response to Borrelia burgdorferi antigens. *Infect. Immun.* **75**, 270-277 (2007).

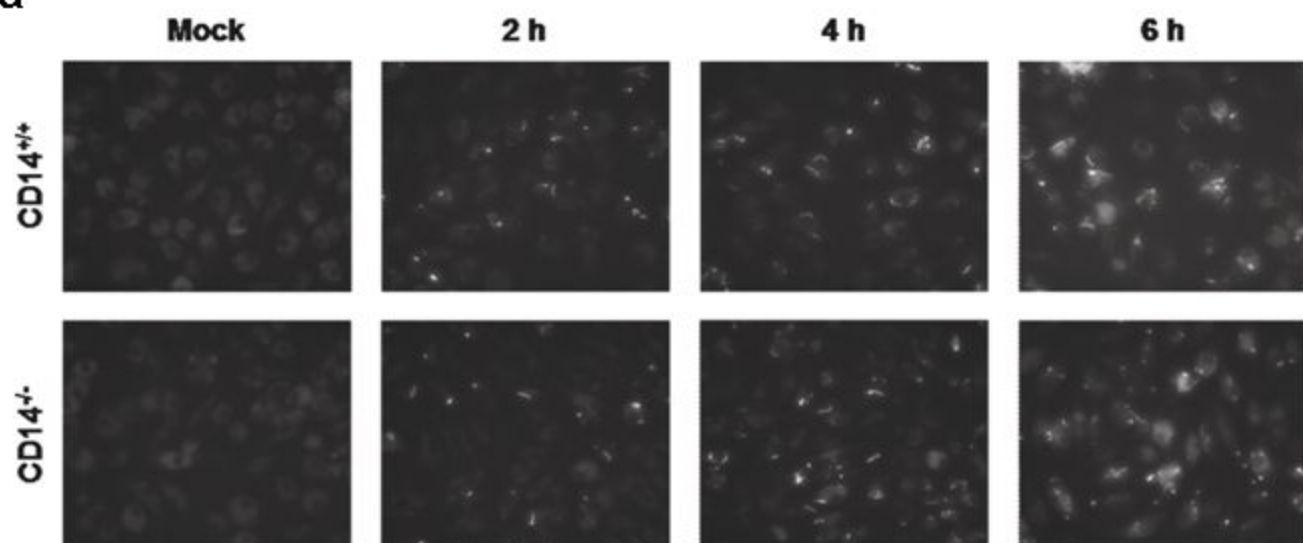
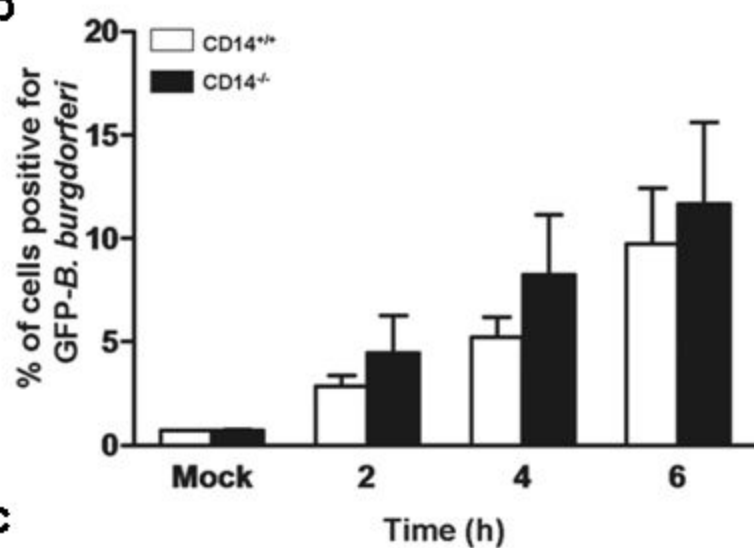
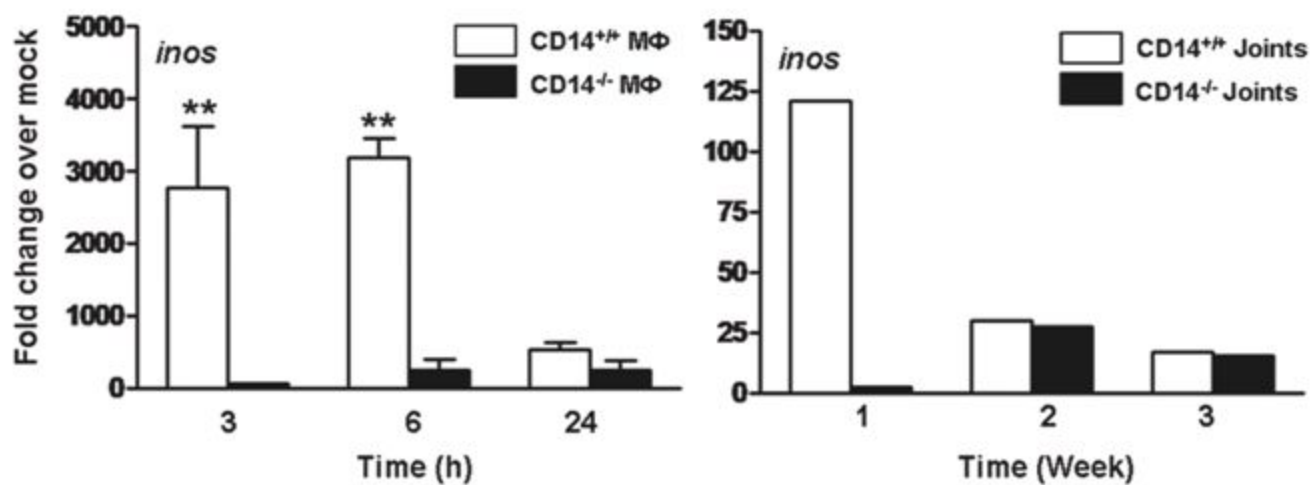
- 1 17. Dean, J.L.E., Sully, G., Clark, A.R., & Saklatvala, J. The involvement of AU-rich element-binding
2 proteins in p38 mitogen-activated protein kinase pathway-mediated mRNA stabilisation. *Cellular*
3 *Signalling* **16**, 1113-1121 (2004).
- 4 18. Bode, J.G. *et al.* The MKK6/p38 mitogen-activated protein kinase pathway is capable of inducing
5 SOCS3 gene expression and inhibits IL-6-induced transcription. *Biol Chem.* **382**, 1447-1453 (2001).
- 6 19. van den Blink, B. *et al.* p38 Mitogen-Activated Protein Kinase Inhibition Increases Cytokine
7 Release by Macrophages In Vitro and During Infection In Vivo. *J Immunol* **166**, 582-587 (2001).
- 8 20. Ogura, H. *et al.* ERK and p38 MAP kinase are involved in downregulation of cell surface TNF
9 receptor 1 induced by acetoxycycloheximide. *Int. Immunopharmacol.* **8**, 922-926 (2008).
- 10 21. Liew, F.Y., Xu, D., Brint, E.K., & O'Neill, L.A. Negative regulation of toll-like receptor-mediated
11 immune responses. *Nat Rev Immunol* **5**, 446-458 (2005).
- 12 22. Saura, M., Zaragoza, C., Bao, C., McMillan, A., & Lowenstein, C.J. Interaction of interferon
13 regulatory factor-1 and nuclear factor kappaB during activation of inducible nitric oxide synthase
14 transcription. *J Mol Biol* **289**, 459-471 (1999).
- 15 23. Saito, H. *et al.* IFN regulatory factor-1-mediated transcriptional activation of mouse STAT-
16 induced STAT inhibitor-1 gene promoter by IFN-gamma. *J Immunol* **164**, 5833-5843 (2000).
- 17 24. Moody, K.D. & Barthold, S.W. Lyme borreliosis in laboratory mice. *Lab Anim Sci* **48**, 168-171
18 (1998).
- 19 25. Schiff, D.E. *et al.* Phagocytosis of gram-negative bacteria by a unique CD14-dependent
20 mechanism. *J. Leukocyte Biol.* **62**, 786-794 (1997).
- 21 26. Steinberg, B.E., Huynh, K.K., & Grinstein, S. Phagosomal acidification: measurement,
22 manipulation and functional consequences. *Biochem Soc. Trans.* **35**, 1083-1087 (2007).
- 23 27. Li, J.D. Exploitation of host epithelial signaling networks by respiratory bacterial pathogens. *J*
24 *Pharmacol. Sci.* **91**, 1-7 (2003).
- 25 28. Chen, G. *et al.* Bacterial endotoxin stimulates macrophages to release HMGB1 partly through. *J*
26 *Leukoc Biol* **76**, 994-1001 (2004).
- 27 29. Moore, M.W. *et al.* Phagocytosis of *Borrelia burgdorferi* and *Treponema pallidum* Potentiates
28 Innate Immune Activation and Induces Gamma Interferon Production. *Infect. Immun.* **75**, 2046-2062
29 (2007).
- 30 30. Cruz, A.R. *et al.* Phagocytosis of *Borrelia burgdorferi*, the Lyme Disease Spirochete, Potentiates
31 Innate Immune Activation and Induces Apoptosis in Human Monocytes. *Infect. Immun.* **76**, 56-70
32 (2008).
- 33 31. Kim, A.H., Khursigara, G., Sun, X., Franke, T.F., & Chao, M.V. Akt Phosphorylates and
34 Negatively Regulates Apoptosis Signal-Regulating Kinase 1. *Mol. Cell. Biol.* **21**, 893-901 (2001).
- 35 32. Ferby, I.M., Waga, I., Sakanaka, C., Kume, K., & Shimizu, T. Wortmannin inhibits mitogen-
36 activated protein kinase activation induced by platelet-activating factor in guinea pig neutrophils. *J.*
37 *Biol. Chem.* **269**, 30485-30488 (1994).

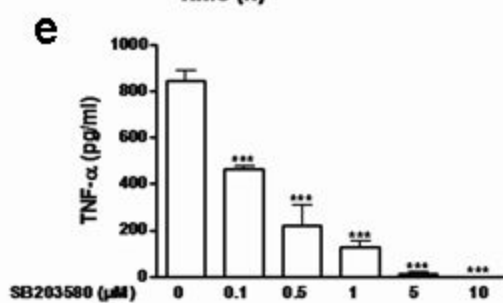
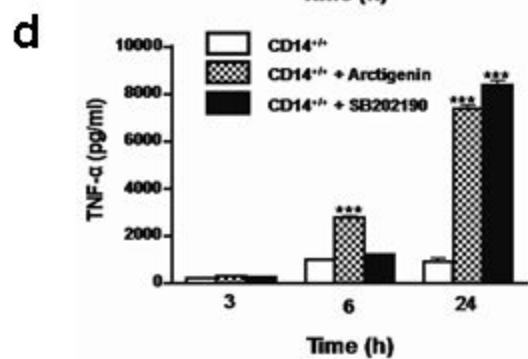
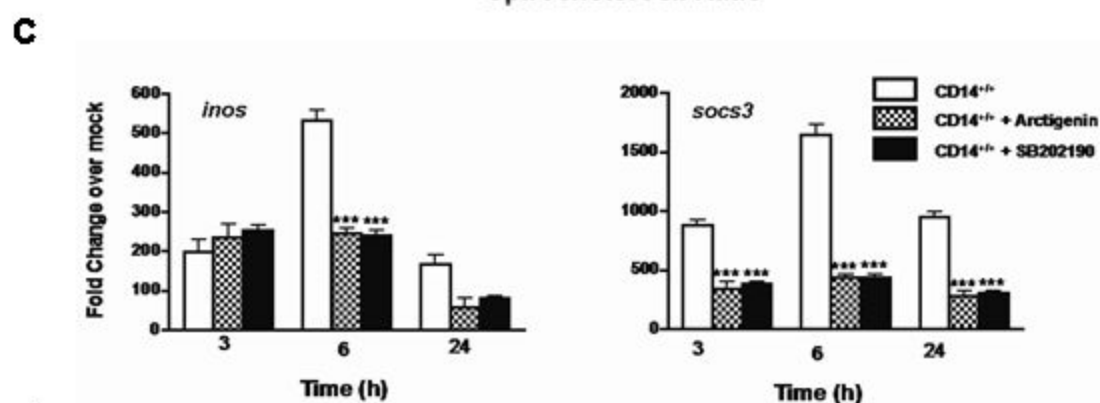
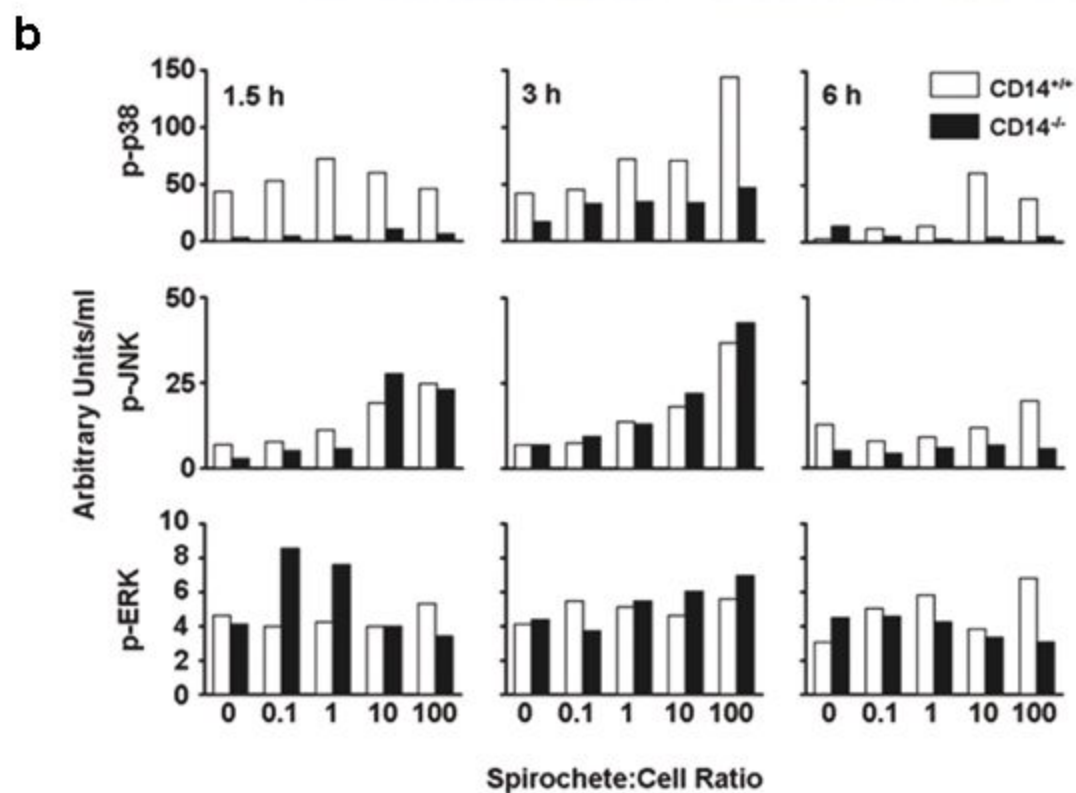
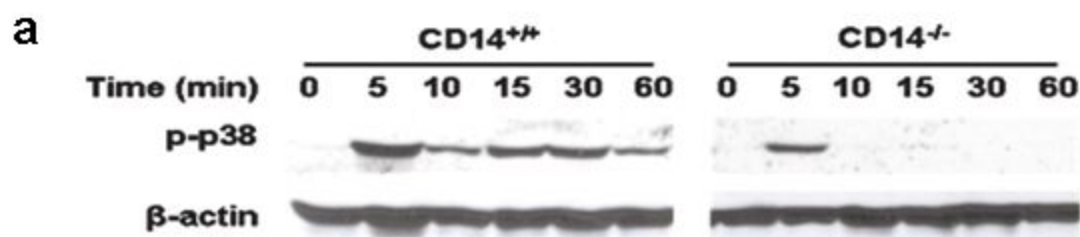
- 1 33. Wooten,R.M. *et al.* Toll-like receptor 2 plays a pivotal role in host defense and inflammatory
2 response to *Borrelia burgdorferi*. *Vector. Borne. Zoonotic. Dis.* **2**, 275-278 (2002).
- 3 34. Lien,E. *et al.* Toll-like Receptor 2 Functions as a Pattern Recognition Receptor for Diverse
4 Bacterial Products. *J. Biol. Chem.* **274**, 33419-33425 (1999).
- 5 35. Wooten,R.M. *et al.* The role of CD14 in signaling mediated by outer membrane lipoproteins of
6 *Borrelia burgdorferi*. *J Immunol* **160**, 5485-5492 (1998).
- 7 36. Wooten,R.M. *et al.* Toll-Like Receptor 2 Is Required for Innate, But Not Acquired, Host
8 Defense to *Borrelia burgdorferi*. *J Immunol* **168**, 348-355 (2002).
- 9 37. Liu,N., Montgomery,R.R., Barthold,S.W., & Bockenstedt,L.K. Myeloid differentiation antigen
10 88 deficiency impairs pathogen clearance but does not alter inflammation in *Borrelia burgdorferi*-
11 infected mice. *Infect. Immun.* **72**, 3195-3203 (2004).
- 12 38. Bolz,D.D. *et al.* MyD88 plays a unique role in host defense but not arthritis development in
13 Lyme disease. *J Immunol* **173**, 2003-2010 (2004).
- 14 39. Moore,K.J. *et al.* Divergent Response to LPS and Bacteria in CD14-Deficient Murine
15 Macrophages. *J Immunol* **165**, 4272-4280 (2000).
- 16 40. Wenneras,C. *et al.* Blockade of CD14 increases *Shigella*-mediated invasion and tissue
17 destruction. *J Immunol* **164**, 3214-3221 (2000).
- 18 41. Matsuzawa,A. *et al.* ROS-dependent activation of the TRAF6-ASK1-p38 pathway is selectively
19 required for TLR4-mediated innate immunity. *Nat Immunol* **6**, 587-592 (2005).
- 20 42. Dib,K. BETA 2 integrin signaling in leukocytes. *Front Biosci.* **5**, D438-D451 (2000).
- 21 43. Sendide,K. *et al.* Cross-talk between CD14 and complement receptor 3 promotes phagocytosis of
22 mycobacteria: regulation by phosphatidylinositol 3-kinase and cytohesin-1. *J Immunol* **174**, 4210-4219
23 (2005).
- 24 44. Hajishengallis,G., Shakhatreh,M.A., Wang,M., & Liang,S. Complement receptor 3 blockade
25 promotes IL-12-Mediated Clearance of *Porphyromonas gingivalis* and Negates Its Virulence In Vivo.
26 *J Immunol* **179**, 2359-2367 (2007).
- 27 45. Koyasu,S. The role of PI3K in immune cells. *Nat Immunol* **4**, 313-319 (2003).
- 28 46. Shouda,T. *et al.* Induction of the cytokine signal regulator SOCS3/CIS3 as a therapeutic strategy
29 for treating inflammatory arthritis. *J Clin. Invest* **108**, 1781-1788 (2001).
- 30 47. Wong,P.K. *et al.* SOCS-3 negatively regulates innate and adaptive immune mechanisms in acute
31 IL-1-dependent inflammatory arthritis. *J Clin. Invest* **116**, 1571-1581 (2006).
- 32 48. Egan,P.J., Lawlor,K.E., Alexander,W.S., & Wicks,I.P. Suppressor of cytokine signaling-1
33 regulates acute inflammatory arthritis and T cell activation. *J Clin. Invest* **111**, 915-924 (2003).
- 34 49. Blander,J.M. & Medzhitov,R. On regulation of phagosome maturation and antigen presentation.
35 *Nat Immunol* **7**, 1029-1035 (2006).

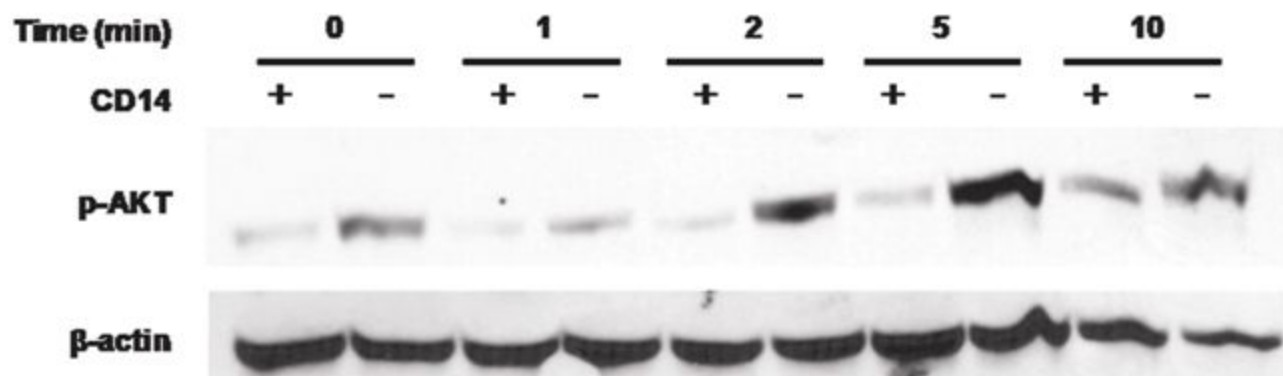
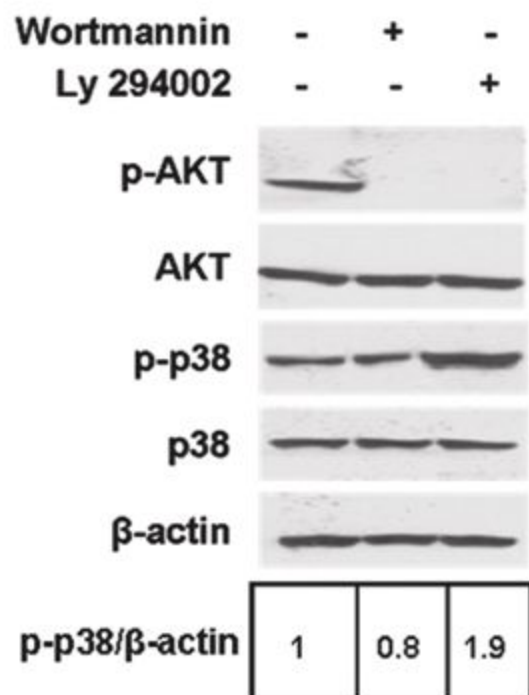
- 1 50. Forman,H.J. & Torres,M. Redox signaling in macrophages. *Mol Aspects Med* **22**, 189-216
2 (2001).
- 3 51. Honda,K. *et al.* Spatiotemporal regulation of MyD88-IRF-7 signalling for robust type-I
4 interferon induction. *Nature* **434**, 1035-1040 (2005).
- 5 52. Decker,T., Muller,M., & Stockinger,S. The Yin and Yang of type I interferon activity in bacterial
6 infection. *Nat Rev Immunol* **5**, 675-687 (2005).
- 7 53. Werts,C. *et al.* Leptospiral lipopolysaccharide activates cells through a TLR2-dependent
8 mechanism. *Nat Immunol* **2**, 346-352 (2001).
- 9 54. Warren,M.K. & Vogel,S.N. Bone marrow-derived macrophages: development and regulation of
10 differentiation markers by colony-stimulating factor and interferons. *J Immunol* **134**, 982-989 (1985).
11
12

a**b****c**

a**b****c**

a**b****c**



a**b****c**